

Possible Involvement of the Vascular Endothelial Growth Factor-Flt-1-Focal Adhesion Kinase Pathway in Chemotaxis and the Cell Proliferation of Osteoclast Precursor Cells in Arthritic Joints¹

Yoshihiro Matsumoto, Kazuhiro Tanaka, Go Hirata, Masuo Hanada, Shuichi Matsuda, Toshihide Shuto, and Yukihide Iwamoto²

Vascular endothelial growth factor (VEGF) plays a crucial role in the pathogenesis of inflammatory joint disease, including angiogenesis and synovitis. Rheumatoid arthritis is a chronic inflammatory disease characterized by progressive synovitis and subsequent bone destruction mediated by osteoclasts (OCs). In this study, we investigate the effects of VEGF on OC precursor cells (pOCs) using Raw cells and adjuvant-induced arthritis in rats. OCs and pOCs in the arthritic joints express VEGF and VEGF receptor type I (Flt-1). Raw cells also express Flt-1, and VEGF treatment stimulated chemotaxis, cell proliferation, the association of Flt-1 with focal adhesion kinase (FAK), and the tyrosine phosphorylation of FAK in Raw cells. The tyrosine phosphorylation of FAK was also observed in pOCs in the arthritic joints of adjuvant-induced arthritis. Adenovirus-mediated expression of FAK-related nonkinase in Raw cells inhibited the effects of VEGF in a dominant negative manner. Furthermore, intra-articular injection of the FAK-related nonkinase virus suppressed the recruitment of pOCs and bone destruction. Our results suggest the possible involvement of the VEGF-Flt-1-FAK pathway in inflammatory disease-induced joint destruction. *The Journal of Immunology*, 2002, 168: 5824–5831.

Vascular endothelial growth factor (VEGF)³ plays a crucial role in the pathogenesis of inflammatory joint diseases, including angiogenesis and synovitis (1). Recent reports have shown that the development of synovitis, a model of rheumatoid arthritis, in collagen-induced arthritis in mouse, can be attenuated with neutralizing anti-VEGF Ab. This suggests the involvement of VEGF signals in arthritic joint destruction (2, 3). Bone resorption mediated by osteoclasts (OCs) in the inflamed joints is a critical part of arthritic joint destruction. Recently, it was demonstrated that VEGF acts as a chemoattractant for OCs and that the invasion of OCs into hypertrophic cartilage requires the presence of VEGF (4). OC precursor cells (pOCs) are recruited from hematopoietic tissue, including bone marrow, via circulating blood. However, the precise process of the recruitment of pOCs into the site of bone resorption remains unclear.

VEGF binds to two tyrosine kinase receptors, Flt-1 and Flk-1, with high affinity (5). While the biological function of the VEGF receptor type II, Flk-1, is understood, that of Flt-1 is still unclear (6). It has been recently reported that VEGF is potentially a monocyte chemoattractant (7) and that monocytes express not Flk-1 but Flt-1 (8). Furthermore, macrophages derived from Flt-1 mutant mice indicated deranged chemotaxis in response to VEGF (9). These findings show that the activation of Flt-1 may stimulate the migration of monocyte/macrophage lineages. However, the signaling pathway of Flt-1 was not yet fully understood.

Focal adhesion kinase (FAK) is a cytoplasmic protein tyrosine kinase that is localized to focal adhesions (10) and involved in the control of several biological processes, including cell spreading, migration, and survival (11). FAK associates with activated growth factor receptors such as platelet-derived growth factor and epidermal growth factor receptors through its N-terminal domain and plays important roles in platelet-derived growth factor-induced and epidermal growth factor-induced cell migration (12). Furthermore, it has been shown that the tubulogenic activity of rat endothelial cells is dependent on the VEGF-Flt-1-FAK pathway (13).

In this study, we tried to elucidate the effects of VEGF on pOCs in vitro and the role of the VEGF signaling pathway in the recruitment of pOCs in rats with adjuvant-induced arthritis (AIA). We demonstrate for the first time the possible involvement of the VEGF-Flt-1-FAK pathway in chemotaxis and the cell proliferation of pOCs in arthritic joint destruction.

Materials and Methods

Agents

Recombinant mouse VEGF was obtained from Genzyme/Techne (Minneapolis, MN). Anti-receptor activators of NF- κ B (RANK), VEGF, Flt-1, and Flk-1 Abs were purchased from Santa Cruz Biotechnology (Santa Cruz, CA). Anti-FAK and phosphotyrosine (clone 4G10) Abs came from Upstate

Department of Orthopedic Surgery, Graduate School of Medical Sciences, Kyushu University, Fukuoka, Japan

Received for publication December 26, 2001. Accepted for publication March 20, 2002.

The costs of publication of this article were defrayed in part by the payment of page charges. This article must therefore be hereby marked *advertisement* in accordance with 18 U.S.C. Section 1734 solely to indicate this fact.

¹ This study was supported in part by grants-in-aid for Scientific Research (12557125 and 10307034) from the Japan Society for the Promotion of Science, and a grant-in-aid for Cancer Research from the Ministry of Health, Labor and Welfare, Japan.

² Address correspondence and reprint requests to Dr. Yukihide Iwamoto, Department of Orthopedic Surgery, Graduate School of Medical Sciences, Kyushu University, 3-1-1 Maidashi, Higashi-ku, Fukuoka 812-8582. E-mail address: yiwamoto@ortho.med.kyushu-u.ac.jp

³ Abbreviations used in this paper: VEGF, vascular endothelial growth factor; OC, osteoclast; pOC, OC precursor cell; MCP-1, monocyte chemoattractant protein-1; MAPK, mitogen-activated protein kinase; PI3K, phosphatidylinositol 3-kinase; moi, multiplicity of infection; AIA, adjuvant-induced arthritis; FAK, focal adhesion kinase; RANK, receptor activator of NF- κ B; FRNK, FAK-related nonkinase; BrdU, 5-bromo-2'-deoxyuridine; TRITC, tetramethylrhodamine isothiocyanate; TRAP, tartrate-resistant acid phosphatase; Pyk2, proline-rich tyrosine kinase 2.

Biotechnology (Lake Placid, NY). Anti-phospho-FAK and proline-rich tyrosine kinase 2 (Pyk2) Abs were from BioSource (Chicago, IL). A cell proliferation ELISA 5-bromo-2'-deoxyuridine (BrdU) kit was purchased from Roche (Mannheim, Germany). PD98059 was obtained from Calbiochem (San Diego, CA), and wortmannin was purchased from Sigma-Aldrich (St. Louis, MO).

Induction of AIA

Induction of AIA was performed as previously described (14). Briefly, 10- to 12-wk-old female Lewis rats (100 g) were injected s.c. with 300 μ l (5 mg/ml) of lyophilized *Mycobacterium butyricum* (Difco, Detroit, MI) at the base of tail. All time points were considered in relation to the AIA induction day, designated as day 0. Arthritis of the bilateral ankle joints was developed in 100% of the treated animals by day 10.

Immunohistochemistry and immunofluorescence

Immunohistochemistry and immunofluorescence were performed as previously described (15). Briefly, joint specimens were initially decalcified for 2 wk in an EDTA-containing buffer and embedded in paraffin. The endogenous peroxidase activity was quenched by incubating the sections in absolute methanol and 3% hydrogen peroxide. The slides were then incubated with various primary Abs. Biotinylated Abs and peroxidase-conjugated streptavidin were used as second and third reagents, respectively. The signals were detected using 3-amino-9-ethylcarbazole in *N,N*-dimethylformamide. The slides were counterstained with methylgreen. For immunofluorescence examination, primary Abs were applied simultaneously and incubated overnight at 4°C. The samples were washed in PBS and incubated with FITC- or tetramethylrhodamine isothiocyanate (TRITC)-conjugated secondary Abs. Then the sections were mounted and examined by confocal laser scanning microscopy.

Cell lines and culture conditions

The mouse myeloid cell line Raw 264.7 was obtained from American Type Culture Collection (Manassas, VA). The cells were maintained in an anti-MEM (Nissui Pharmaceutical, Tokyo, Japan) supplemented with 100 U/ml penicillin, 100 μ g/ml streptomycin, and 10% FBS. The cells were incubated at 37°C in a humidified atmosphere with a CO₂ content of 5%. The cells were harvested by scraping, counted using a hemocytometer, and then used for various experiments.

Immunoprecipitation and immunoblotting

Cells that were growing logarithmically ($2-4 \times 10^6$) at ~70% confluency were harvested and solubilized in a lysis buffer (20 mM Tris (pH 7.4), 250 mM NaCl, 1.0% Nonidet P-40, 1 mM EDTA, 50 mg/ml leupeptin, and 1 mM PMSF). Protein quantity was determined with a Bradford protein assay (Bio-Rad, Hercules, CA). The protein samples were boiled for 5 min, and 10 μ g of total protein from each sample was run on 4–12% gradient pre-cast MOPS-polyacrylamide gels (NOVEX, San Diego, CA) and blotted onto a nitrocellulose filter. For immunoprecipitations, lysate aliquots were incubated with anti-FAK Ab overnight at 4°C. Immunocomplexes were collected on protein A-G Sepharose beads (Santa Cruz Biotechnology). The beads were washed three times with a lysis buffer, boiled, and subjected to electrophoresis. After transfer to nitrocellulose membranes, the filters were pretreated with TBS containing 5% dry milk and 0.05% Triton X for 2 h at room temperature. They were then incubated with the appropriate primary Abs for 2 h at room temperature. After several washes, a HRP-conjugated secondary Ab (BioSource) was added and incubated at room temperature for 1 h. After the final wash, the immunoreactivity of the blots was detected using an ECL system (Amersham, Arlington Heights, IL).

Cell proliferation assay

Raw cells seeded in culture plates were incubated in serum-free medium with or without VEGF for 24 h. The cell growth rate was determined using a cell proliferation kit (Roche) based on the ELISA for a thymidine analog, BrdU, according to the manufacturer's protocol.

Chemotaxis assay

The chemotaxis assay was performed using transwell chambers (Costar, Cambridge, MA) as described previously (16–18). In brief, cells were suspended in serum-free anti-MEM containing 1% BSA and seeded in the upper chamber. The lower chamber was filled with serum-free anti-MEM, which was or was not supplemented with various cytokines (10 ng/ml VEGF, 10 ng/ml TNF- α , 500 pg/ml IL-1 α , 10 ng/ml M-CSF, and 10 ng/ml monocyte chemoattractant protein-1 (MCP-1)). Polyvinylpyrrolidone-free polycarbonate filters with 8- μ m pore size were coated with type IV col-

lagen and inserted between the two chambers. Then the cells were allowed to migrate for 6 h at 37°C. After the incubation, cells that migrated to the lower side of the filter were fixed, stained, and counted for five fields per filter under a microscope.

Flow cytometry

Cells were washed with ice-cold PBS twice and harvested by scraping. The cells were then stained with anti-Flt-1 or Flk-1 Abs. The stained cells were further incubated with FITC-conjugated secondary Abs and analyzed using a flow cytometer (FACSCalibur; BD Biosciences, San Jose, CA).

Adenoviral constructs

A replication-defective adenovirus encoding FAK-related nonkinase (FRNK), Adv-FRNK, was kindly provided by Dr. A. M. Samarel (19). A replication-defective adenovirus containing the β -galactosidase gene, LacZ (Adv-LacZ), was used to control for the nonspecific effects of viral infection. Adenoviruses were amplified and purified using HEK293 cells, as previously described (20). Preliminarily, it was determined that a viral concentration of >10 multiplicity of infection (moi) produced a detectable expression of FRNK protein within 48 h. The infected cells were subjected to immunoblotting, chemotaxis, and cell proliferation assays.

Assessment of the effect of Adv-FRNK on AIA

Twenty-one rats were immunized with adjuvant (day 0). On days 7 and 14, PBS ($n = 7$), LacZ ($n = 7$), and FRNK ($n = 7$) mice were intra-articularly injected with 50 μ l of PBS, adv-LacZ, and adv-FRNK, respectively. The viruses (1×10^8 virus particles per joint) were directly injected into the bilateral joint spaces. On days 7, 14, 21, and 28, hind paws were immersed into the chamber up to the anatomic hair line and edema measurement were made with a volumetric apparatus (MK-550; Muromachi-kikai, Tokyo, Japan). On days 21 and 28, the rats were sacrificed and the therapeutic effects of Adv-FRNK injection were examined. For histological evaluation, the specimens were fixed and decalcified in 10% EDTA for 14 days and embedded in paraffin. The sectioned specimens were subjected to tartrate-resistant acid phosphatase (TRAP) staining and immunohistochemistry. The number of TRAP-positive cells was calculated in three sections of ankle joints from three different specimens in each group. Five visual fields were randomly selected in each section and the number of TRAP-positive cells was counted under a microscope. For radiological examination, both hind paws were dissected on day 28 and examined by soft x-ray (Softex, Tokyo, Japan). The evaluations were performed blindly by the same observer. A 0–3 subjected grading scale (0 = normal, 1 = mild, 2 = moderate, 3 = severe) described previously (21), with modification, was used to evaluate four different parameters including joint space narrowing, subchondral bone erosion, osteoporosis, and periosteal new bone formation. The radiological score refers to the sum of the subjective scores for each of these four parameters (maximum 12).

Statistical analysis

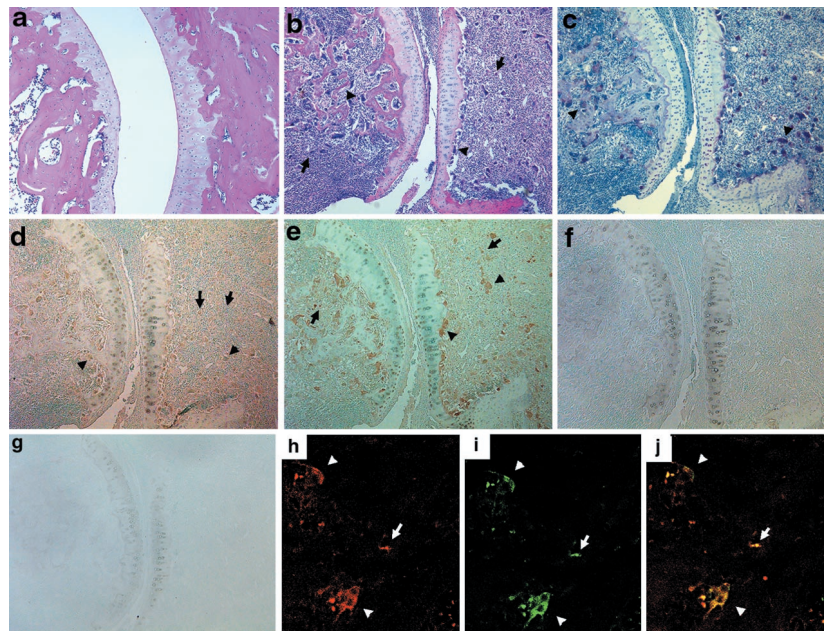
The values of chemotaxis and cell proliferation assays were expressed as the mean \pm SD and were statistically analyzed by a Student's *t* test. The volume of the hind paw volume, the number of TRAP-positive cells, and the radiological scores were analyzed by Mann-Whitney *U* test.

Results

Expression of VEGF and VEGF receptors at the site of bone destruction in rats with AIA

Initially, we analyzed the expression profiles of VEGF and VEGF receptors in the specimens taken from the ankle joints of rats with AIA. Arthritis was remarkably induced in the hind feet of the rats ~3 wk after immunization by adjuvants. The specimens of ankle joints showed strong bone destruction and the accumulation of mononuclear (Fig. 1*b*, arrows) and multinuclear cells (Fig. 1*b*, arrowheads). TRAP staining demonstrated the presence of bone-resorbing OCs (Fig. 1*c*, arrowheads). In serial sections, expressions of VEGF and Flt-1 were observed mainly in infiltrating mononuclear cells (Fig. 1, *d* and *e*, arrows) and TRAP-positive multinuclear cells (Fig. 1, *d* and *e*, arrowheads) that were near the bone surface. Flk-1 expression was not found in the same cells (Fig. 1*f*). Tissue sections stained with preimmune control IgG showed no nonspecific staining (Fig. 1*g*). Because mature OCs and pOCs expressed RANK (22), we next investigated whether Flt-1

FIGURE 1. Expression of VEGF and VEGF receptors in arthritic joints. Control normal rats (*a*) and rats immunized with adjuvant (*b–f*) were sacrificed on day 21, and serial sections of the ankle joints were prepared. The sections were stained with H&E (*a* and *b*), TRAP (*c*), and Abs against VEGF (*d*), Flt-1 (*e*), Flk-1 (*f*), or control IgG (*g*). Arrowheads indicate multinuclear cells and arrows indicate surrounding mononuclear cells. Original magnification: $\times 100$. For the immunofluorescence, the serial sections were prepared as above and stained with anti-RANK (*h*) and anti-Flt-1 (*i*) Abs, followed by secondary Abs conjugated with TRITC and FITC, respectively. Both images were merged (*j*). Arrowheads indicate multinuclear cells and arrowheads indicate surrounding mononuclear cells.



was colocalized with RANK-positive cells in the AIA joints. The specimens were incubated with anti-RANK (Fig. 1*h*) and anti-Flt-1 (Fig. 1*i*) Abs and then reacted with TRITC- or FITC-labeled secondary Abs, respectively. As shown in Fig. 1*j*, RANK and Flt1 were colocalized in mononuclear (Fig. 1*j*, arrow) and multinuclear (Fig. 1*j*, arrowheads) cells in the specimens. These results suggest that OCs and pOCs in the AIA joints expressed Flt-1.

Expression of Flt-1 in Raw cells, a model of pOCs

We next focused on the involvement of VEGF signaling in pOCs in vitro. The myeloid Raw cells in mice have been shown to be able to differentiate into OC-like cells in the presence of RANK ligand (23, 24). In this study, treatment of Raw cells with RANK ligand (100 ng/ml) for 6 days induced the formation of multinuclear TRAP-positive OC-like cells, and the cells were able to form resorption pits on dentin slices (data not shown). Raw cells also expressed CD11b, which is a typical marker of macrophages (data not shown), indicating that Raw cells are in the same lineage as monocyte-macrophage and can be used as pOCs. FACS analysis demonstrated that Raw cells expressed Flt-1, but not Flk-1 (Fig. 2*a*). Expression of VEGF was also observed in the cells (data not shown). Because tyrosine phosphorylation was required to activate Flt-1, we next examined the tyrosine phosphorylation of Flt-1 in Raw cells after treatment with VEGF. As shown in Fig. 2*b*, Flt-1 was tyrosine-phosphorylated by VEGF treatment, and the neutralizing Ab against VEGF effectively inhibited the phosphorylation of Flt-1.

Effect of VEGF treatment on chemotaxis and the cell proliferation of Raw cells

Adding VEGF to the lower chamber stimulated the chemotaxis of Raw cells, and maximal stimulation was observed at 10 ng/ml with a typical bell-shaped curve. VEGF-driven chemotaxis was inhibited by the neutralizing Ab to VEGF (Fig. 3*a*). However, other bone-resorptive cytokines such as TNF- α , IL-1 α , and M-CSF could not enhance the chemotaxis of Raw cells. However, the addition of serum or MCP-1 to the lower chamber enhanced the chemotaxis, as previously reported (25) (Fig. 3*b*). We next analyzed the VEGF-induced cell proliferation of Raw cells by using BrdU incorporation assay. Stimulation of serum-starved Raw cells

with various concentrations of VEGF for 24 h raised the cell proliferation dose-dependently in contrast to serum-free control cells (Fig. 3*c*). VEGF (50 ng/ml) stimulated the cell proliferation of Raw cells at a level ~ 3 -fold higher that of control cells. TNF- α , IL-1, and M-CSF also stimulated the cell proliferation of Raw cells (Fig. 3*d*). These results indicate that VEGF enhanced the chemotaxis and cell proliferation of Raw cells.

Tyrosine phosphorylation of FAK induced by VEGF

VEGF binds to its plasma membrane receptors and transmits signals through the phosphorylation of intracellular proteins. After

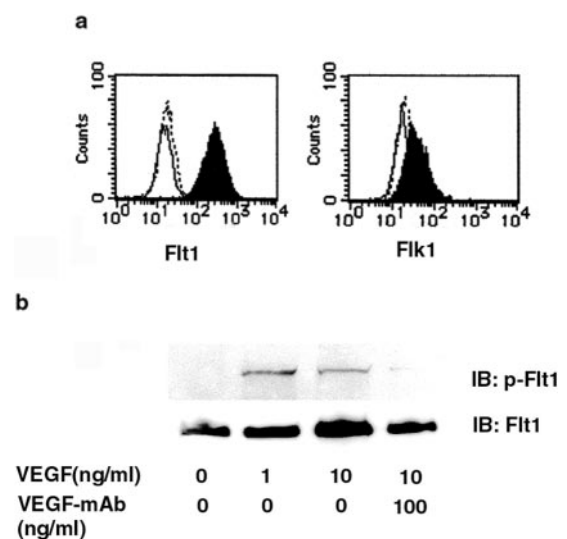


FIGURE 2. Expression of Flt-1 in Raw cell models of pOCs. *a*, Flow cytometric analysis of the expression profiles of VEGF receptor in Raw cells. The cells were reacted with anti-Flt-1 and Flk-1 Abs and then with FITC-conjugated secondary Abs. They were then analyzed using flow cytometry. *b*, Tyrosine phosphorylation of Flt-1 in response to VEGF. Raw cells were cultured in a serum-free medium overnight and then exposed to various concentrations of VEGF with or without a neutralizing Ab (100 ng/ml) for 10 min. The cell lysates were subjected to SDS-PAGE, and the filters were immunoblotted with anti-tyrosine phosphorylated Flt-1 Abs (upper panel) and anti-Flt-1 Abs (lower panel).

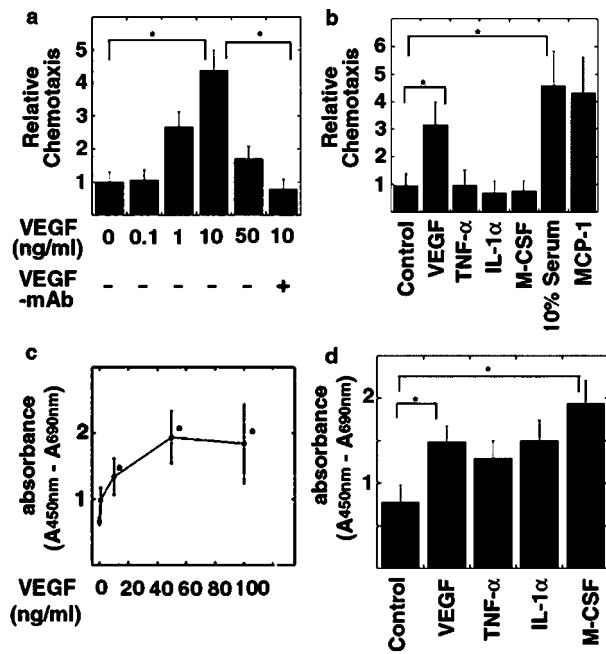


FIGURE 3. Stimulation of chemotaxis and cell proliferation of Raw cells by VEGF. *a*, Raw cells were cultured in a serum-free medium overnight and washed with PBS twice. The cells were added into the upper compartment of a modified Boyden chamber. The indicated concentrations of VEGF were added to the lower compartments with or without a neutralizing Ab to VEGF (100 ng/ml). The chambers were incubated for 6 h at 37°C, and then cells that had migrated were stained and counted as described in *Materials and Methods*. The results show the mean \pm SD. *b*, VEGF (10 ng/ml) and inflammatory cytokines (10 ng/ml TNF- α , 500 pg/ml IL-1 α , 10 ng/ml M-CSF, and 10 ng/ml MCP-1 or 10% serum) were added to the lower compartments and chemotaxis assay was conducted. Results show the mean \pm SD of three independent experiments (*, $p < 0.01$). *c*, Raw cells in a 96-well plate were cultured in a serum-free medium for 24 h and washed with PBS. Then the cells were stimulated with the indicated concentrations of VEGF for 24 h. Thereafter, BrdU was added to the medium and incubated for another 2 h. Incorporation of BrdU into the cells was determined by ELISA. Results show the mean \pm SD of three independent experiments. *d*, Raw cells were also stimulated with various inflammatory cytokines (50 ng/ml VEGF, 10 ng/ml TNF- α , 500 pg/ml IL-1 α , and 100 ng/ml M-CSF), and the incorporation of BrdU into the cells was analyzed. Results show the mean \pm SD of three independent triplicated experiments (*, $p < 0.01$).

VEGF treatment, major tyrosine-phosphorylated bands were found at 180 to \sim 200 kDa and 110 to \sim 130 kDa in size (data not shown). It was reported that 112-kDa Pyk2, a member of the FAK family, acts to transmit biological signals such as cell adhesion and bone resorption in mature OCs (26). Therefore, we first postulated that VEGF treatment might induce tyrosine phosphorylation of Pyk2. However, Raw cells showed constitutive phosphorylation of Pyk2, and VEGF treatment did not affect the phosphorylation (Fig. 4*a*).

FAK, a 125-kDa protein, is also reported to be expressed in human peripheral monocytes (27). When Raw cells were stimulated by VEGF (10 ng/ml) for 10 min, the amount of Flt-1 that bound to FAK was increased by \sim 5- to 6-fold compared with that of the control, suggesting a VEGF-induced association between Flt-1 and FAK (Fig. 4*b*). We then investigated the effect of VEGF in the tyrosine phosphorylation of FAK. VEGF treatment induced the tyrosine phosphorylation of FAK in Raw cells, and the neutralizing Ab reduced the phosphorylation (Fig. 4*c*). It has been reported that major sites of FAK phosphorylation are tyrosine residues 397, 576, 577, 861, and 925 (28), and that each residue has

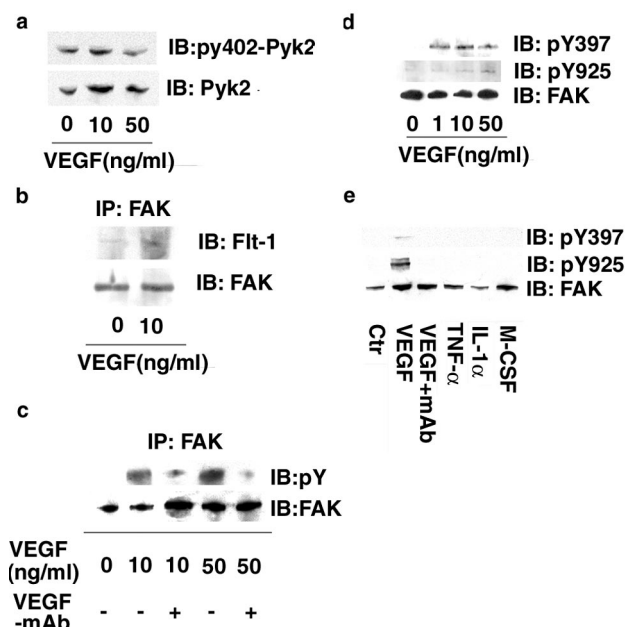


FIGURE 4. Induction of the tyrosine phosphorylation of FAK in Raw cells. Raw cells were cultured in a serum-free medium overnight. Then the cells were washed and incubated for 5 min in the presence of various concentrations of VEGF with or without a neutralizing Ab (100 ng/ml). The samples were then immunoblotted with anti-phosphorylated Pyk2 Ab reacting with the tyrosine residue at 402 (pY402-Pyk2) and anti-Pyk2 Abs (*a*). The same samples were immunoprecipitated with anti-FAK Ab, and the precipitants were immunoblotted with anti-Flt1 and anti-FAK Abs (*b*) or anti-pY and anti-FAK Abs (*c*). The precipitants were also immunoblotted with anti-phosphorylated FAK Abs reacted with the tyrosine residue at 397 (pY397-FAK), tyrosine residue at 925 (pY925-FAK), or anti-FAK Abs (*d*). Raw cells were stimulated by various inflammatory cytokines (10 ng/ml VEGF, 10 ng/ml VEGF plus 100 ng/ml neutralizing Ab to VEGF, 10 ng/ml TNF- α , 500 pg/ml IL-1 α , and 100 ng/ml M-CSF). The samples were subjected to immunoblot analysis using anti-pY397, anti-pY925-FAK, and anti-FAK Abs (*e*).

a specific function (29). After VEGF stimulation, we observed the tyrosine phosphorylation of Y397 and Y925 (pY397 and pY925) in FAK (Fig. 4*d*), whereas no tyrosine phosphorylation was observed in Y576, Y577, and Y861 (data not shown). Other cytokines involved in pathological bone resorption, such as IL-1 α , TNF- α , and M-CSF, did not induce the phosphorylation of FAK (Fig. 4*e*). In the joints of rats with AIA, the expressions of pY397 in FAK were also observed in the small mononucleated cells near the bone surface (Fig. 5*b*, arrows), while control IgG Ab showed no nonspecific staining (Fig. 5*c*). The expression pattern of pY925 in FAK was similar to that of pY397 (data not shown). Immunofluorescence analysis clearly indicated that small RANK-positive cells, probably pOCs, expressed pY397 in FAK (Fig. 5, *d-f*, arrows).

Involvement of PI3K and MAPK downstream on the VEGF-Flt-1-FAK pathway

Y397 in FAK has been identified as the binding site for phosphatidylinositol 3-kinases (PI3K) and functions as a critical factor for cell motility (30). In this study, pretreatment of Raw cells with wortmannin, a specific inhibitor of PI3K, reduced VEGF-driven chemotaxis (Fig. 6*a*), indicating that PI3K might be involved in VEGF-Flt-1-FAK signaling in the cells. Recently it was demonstrated that pY925 in FAK creates a binding site for the SH2 domain of Grb2 (31), and that this interaction may activate the Ras-extracellular signal-regulated kinase/mitogen-activated protein

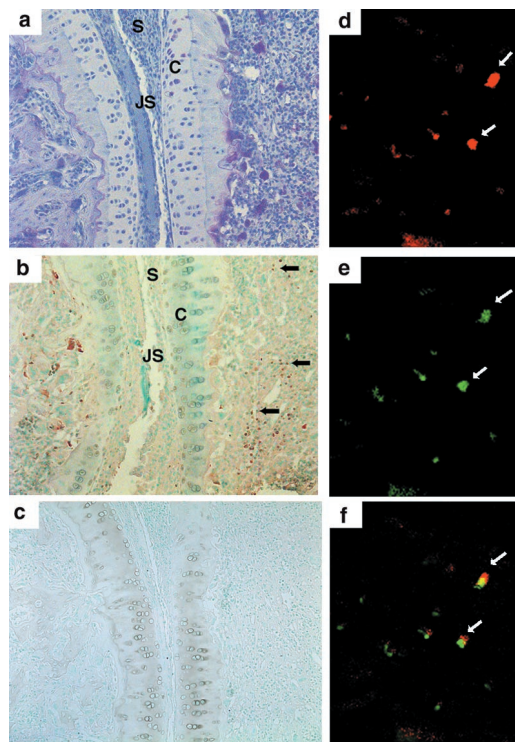


FIGURE 5. Expression of pY397-FAK in the inflamed joints of rats with AIA. Rats with AIA were sacrificed on day 21, and the serial sections of ankle joints were prepared. The sections were stained with TRAP (a), anti-pY397-FAK Abs (b), and control IgG (c). Arrows indicate the small, round cells expressing pY397-FAK. S, Synovium; C, cartilage; JS, joint space. Original magnification: $\times 200$. For the immunofluorescence, the serial sections were prepared as above and stained with anti-RANK (d) and anti-pY397-FAK Abs (e), followed by secondary Abs conjugated with TRITC and FITC, respectively. Both images were merged (f). Arrows indicate small cells, probably pOCs.

kinase (MAPK) pathway (32). In the present study, PD98059, a specific MAPK inhibitor, reduced the VEGF-induced cell proliferation in a dose-dependent manner (Fig. 6b), suggesting the involvement of the MAPK pathway in the VEGF-induced cell proliferation of pOCs.

Effect of FRNK infection in Raw cells

To further examine the role of FAK in the VEGF-driven chemotaxis and the cell proliferation of Raw cells, we inhibited the function of FAK by using a replication-defective adenovirus which contained FRNK (adv-FRNK). Initially, Raw cells were infected with adenovirus containing β -galactosidase (adv-LacZ). X-gal staining revealed that $>95\%$ of the cells were effectively infected with adv-LacZ (moi = 10) (data not shown). When Raw cells were infected with adv-FRNK (moi = 10), the cells expressed FRNK (Fig. 7a). The FRNK-infected cells exhibited a decreased basal level of chemotaxis compared with control cells. Furthermore, the cells expressing FRNK did not respond to VEGF treatment (Fig. 7b). Infection by adv-FRNK also remarkably reduced VEGF-induced cell proliferation. However, adv-FRNK failed to inhibit the M-CSF-stimulated proliferation of Raw cells (Fig. 7c). Adv-FRNK also abrogated the phosphorylation of Y397 and Y925 in FAK induced by VEGF (Fig. 7d). The expression of total FAK was not affected by the infection of viruses (data not shown).

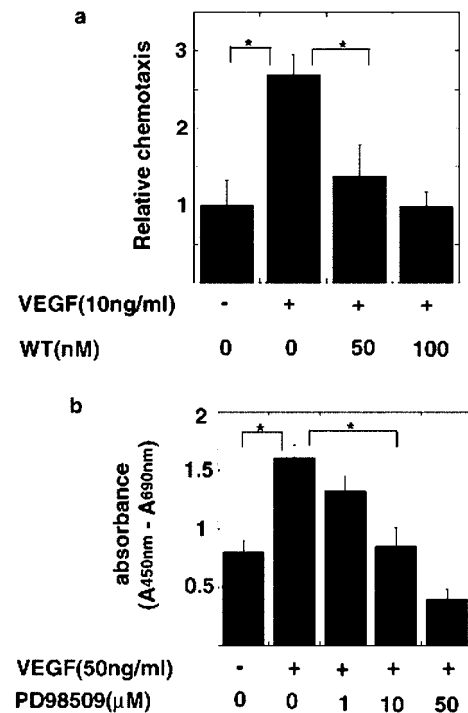


FIGURE 6. Possible involvement of PI3K and MAPK downstream in the Flt-1-FAK pathway. a, The cells were incubated with indicated concentrations of wortmannin (WT) for 6 h. Then the cells were added into the upper compartments of a modified Boyden chamber. The indicated concentrations of VEGF (10 ng/ml) were added to the lower compartments and incubated for 6 h at 37°C. The cells that migrated were stained and counted as described in the *Materials and Methods*. Results show the mean \pm SD of three independent experiments (*, $p < 0.01$). b, Raw cells were incubated with various concentrations of PD98059 in the presence of VEGF (50 ng/ml) for 24 h. Then BrdU was added to the cultures and incubated for another 2 h. Incorporation of BrdU into the cells was determined by ELISA. Results show the mean \pm SD of three independent triplicated experiments (*, $p < 0.01$).

Possible involvement of the VEGF-Flt1-FAK pathway in bone destruction in AIA rats

The results described above indicate that the activation of the VEGF-Flt-1-FAK pathway may play an important role in infiltrating the pOCs in the arthritic joints of rats with AIA. To obtain direct evidence to support this notion, we injected Adv-FRNK into the inflamed ankle joints of rats with AIA. On day 21, histopathologic examination of the joints from rats treated with adv-FRNK showed suppressed infiltration of mononuclear and multinuclear cells (Fig. 8b) compared with those with adv-LacZ (Fig. 8a). In addition, the number of the mononuclear cells with the expression of pY397 in FAK (Fig. 8d, arrows) was notably reduced through treatment with adv-FRNK, but not with adv-LacZ (Fig. 8c). The serial sections stained with control anti-IgG Ab showed no non-specific signaling (Fig. 8, e and f). The expression of FRNK proteins in the joints was confirmed 7 days after the injection (Fig. 8g). On days 21–28, the hind paw volume of AIA rats was also decreased by adv-FRNK (Fig. 8h). Injection of adv-FRNK reduced the number of TRAP-positive cells in the arthritic joints found on day 28 (Fig. 8i). Evaluation by radiological scores on day 28 confirmed that the injection of adv-FRNK significantly reduced joint destruction compared with PBS and adv-LacZ injections (Fig. 8j).

Discussion

The osteoclastic bone destruction in inflamed joints is a sequence of pathological conditions; pOCs are recruited to the site of inflammation, then proliferation and, finally, differentiation of OCs occur in

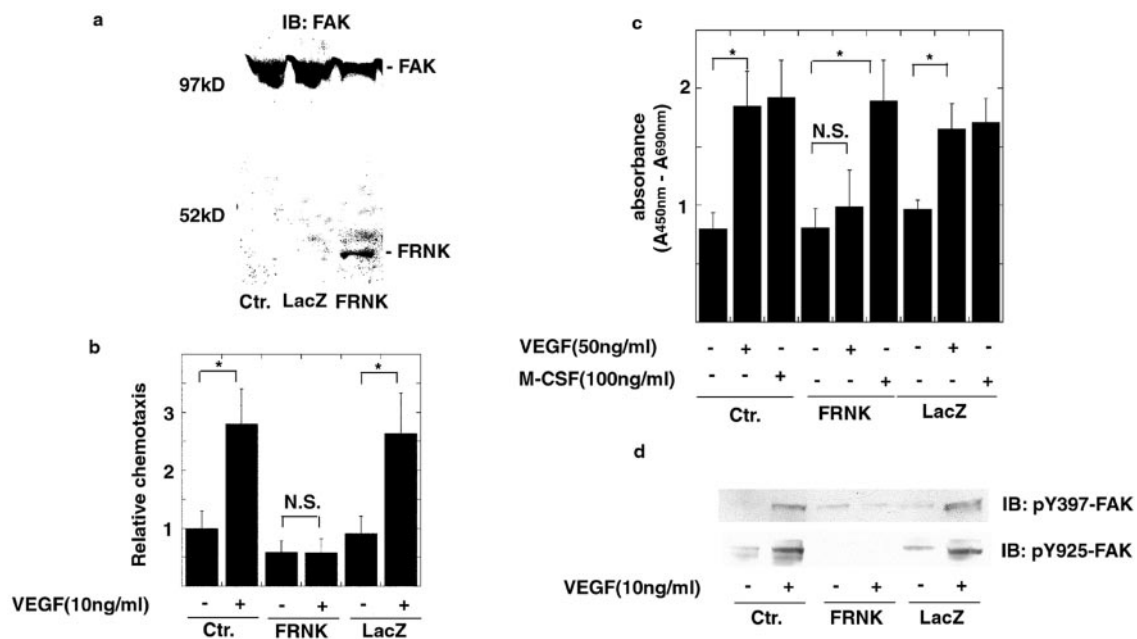


FIGURE 7. Effects of FRNK on the tyrosine phosphorylation of FAK, chemotaxis, and the proliferation of Raw cells. *a*, Raw cells were infected with adv-FRNK or adv-LacZ ($\text{moi} = 10$). Equal amounts of extracted cell lysates were immunoblotted using an Ab that recognized both FAK and FRNK. *b*, The control cells (Ctr.) and infected cells ($\text{moi} = 10$) were subjected to chemotaxis assay using VEGF (10 ng/ml) as a chemoattractant. Results show the mean \pm SD of two independent experiments (*, $p < 0.01$; NS). *c*, The control and infected cells were incubated with VEGF (50 ng/ml) and M-CSF (100 ng/ml) for 24 h. Incorporation of BrdU into the cells was analyzed by ELISA. Results show the mean \pm SD of three independent triplicated experiments (*, $p < 0.01$; NS). *d*, The control and infected cells were maintained in a serum-free medium overnight and then stimulated with VEGF (10 ng/ml) for 10 min. The cell lysates were immunoblotted with anti-pY397 and anti-pY925-FAK Abs.

bone where pOCs fuse to form mature OCs under close contact with osteoblasts/stromal cells (33). VEGF, a stimulator of angiogenesis, is known to play a crucial role in the pathogenesis of rheumatoid arthritis by inducing neovascularization in the pannus (34). Recently, it was also shown that VEGF is a potent chemoattractant for monocytes (7) and that pOCs are cells of monocyte/macrophage lineage (33). Therefore, we postulated that VEGF may play an important role in the recruitment of pOCs by promoting their chemotactic activity. In the present study, we found that the immunolocalization of VEGF, Flt-1, and RANK was mainly associated with the infiltrating mononuclear small round cells and polynuclear giant cells in AIA joints, suggesting that the cells are pOCs and mature OCs.

Inflammatory cytokines such as TNF- α , IL-1 α , and M-CSF are involved in the progression of bone destruction (35–37). However, the effect of these cytokines on the chemotaxis of pOCs remains unclear. Our data demonstrated that VEGF and MCP-1 stimulated the chemotaxis of Raw cells, whereas TNF- α , IL-1 α , and M-CSF did not. Therefore, we concluded that one of the characteristic biological effects of VEGF on pOCs might be the stimulation of chemotaxis in pOCs. Most signals for VEGF-induced cell proliferation of endothelial cells are mediated by Flk-1 (38). In contrast, VEGF treatment caused the phosphorylation of Flt-1 but not Flk-1 and subsequently stimulated the cell proliferation of Raw cells as well as M-CSF, TNF- α , and IL-1 α , pointing to a new function of Flt-1 in pOCs.

The kinase activity of FAK is negatively regulated by FRNK via the dephosphorylation of the tyrosine residues of FAK. Adenoviral expression of FRNK effectively inhibited VEGF-induced chemotaxis, cell proliferation, and the tyrosine phosphorylation of FAK in Raw cells. These results directly demonstrate that tyrosine phosphorylation of FAK was required for the biological effects of VEGF in Raw cells. Inflammatory cytokines such as TNF- α , IL-1 α , and M-CSF did not stimulate the tyrosine phosphorylation of FAK. Therefore, the results suggest that VEGF specifically causes the tyrosine phosphorylation of FAK via Flt-1 in Raw cells to occur.

It was reported that, in HUVECs, FAK plays an important role in VEGF-induced antiapoptosis (39). Thus, it is reasonable to suppose that the VEGF-Flt-1-FAK pathway may mediate an antiapoptotic signal in Raw cells and that dephosphorylation of FAK by FRNK induces apoptosis of the cells. We first infected Raw cells with adv-FRNK or adv-LacZ ($\text{moi} = 10$) under serum-free conditions with or without VEGF (50 ng/ml) for 24 h. Then cell viability was evaluated by a trypan blue dye exclusion assay. However, cell viability was unchanged by the adv-FRNK infection, and addition of VEGF in the medium did not affect the results. We also conducted a DNA fragmentation assay and confirmed that the adv-FRNK infection did not result in DNA fragmentation (data not shown). As shown in Fig. 6, the MAPK pathway may be involved in the VEGF signaling in Raw cells. Consistent with these findings, FRNK effectively reduced VEGF-induced extracellular signal-regulated kinase activation in the cells (data not shown). Taken together, our results suggest that FRNK exerts its inhibitory effect on cell proliferation by attenuating the MAPK activation but not stimulating apoptosis of the cells.

Immunohistochemistry demonstrated that pY397 in FAK was found mainly in pOCs. Using adv-LacZ, we confirmed that the adenovirus vector can effectively transduce the gene at the site of bone destruction in AIA (data not shown), as previously reported (40). Adv-FRNK injection into the arthritic joints decreased the expression of pY397 in FAK as well as the number of OCs in the specimens, resulting in the reduction of bone destruction. These results suggest that the major targets of adv-FRNK might be pOCs and that adv-FRNK inhibited recruitment and proliferation of pOCs in the inflamed joints. Our present findings support the idea that the VEGF-Flt1-FAK pathway might be involved in the bone destruction associated with AIA. However, in the human monocytic cell line THP-1, integrin-dependent cell adhesion to extracellular matrices such as fibronectin causes a rapid tyrosine phosphorylation of FAK (41). The synovial pannus was rich in fibronectin, which could activate FAK in the

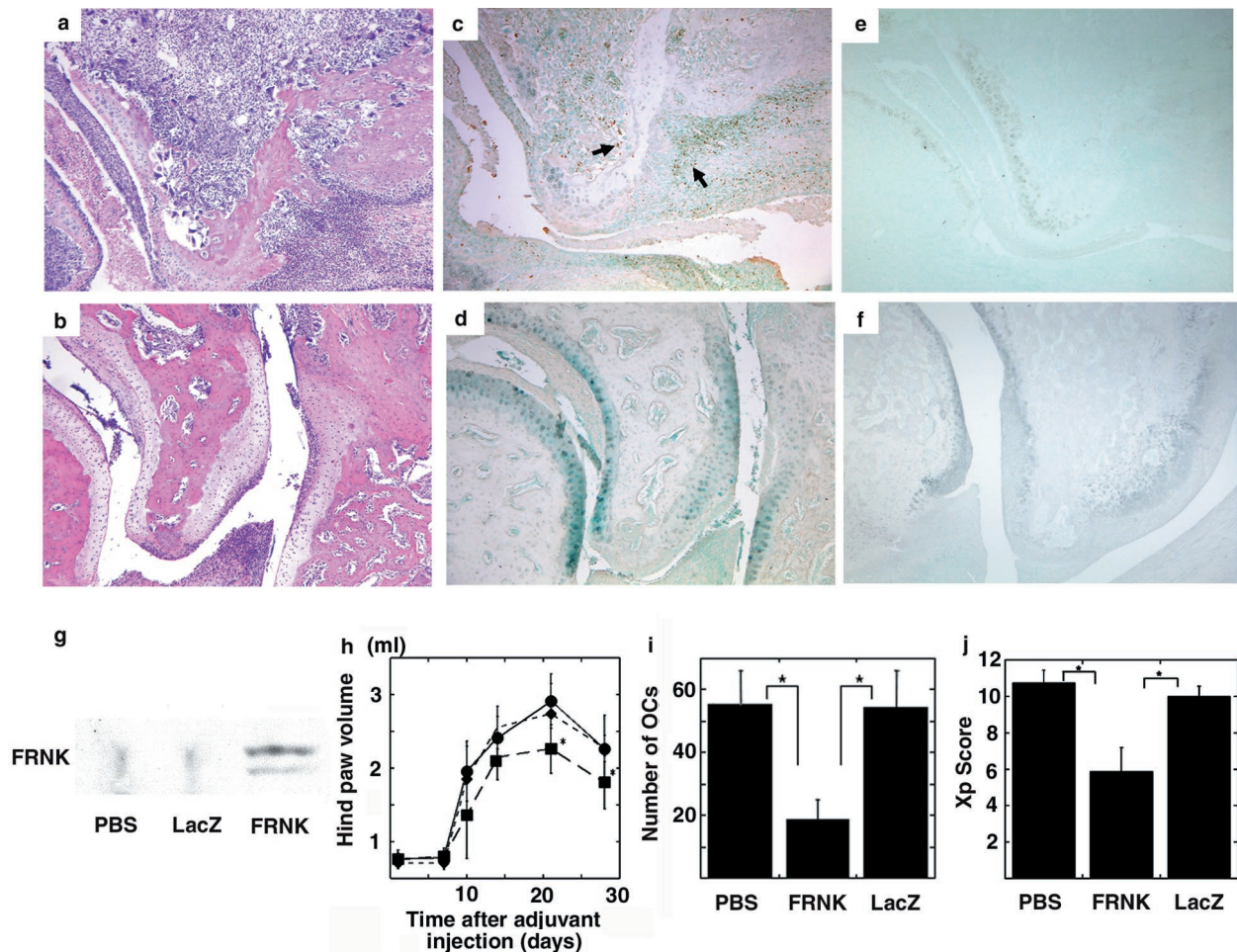


FIGURE 8. Effect of FRNK expression on the progression of AIA. *a-f*, Rats were immunized in the base portion of the tail with adjuvant (day 0), and viruses (adv-FRNK and adv-LacZ) were injected intra-articularly into both ankles on days 7 and 14. Rats were sacrificed, and the ankle joints were fixed on day 21. The specimens were subjected to H&E staining (*a*, LacZ-injected rat; *b*, FRNK-injected rat) and immunohistochemistry using anti-pY397-FAK Abs (*c*, LacZ-injected rat; *d*, FRNK-injected rat) or control IgG (*e*, LacZ-injected rat; *f*, FRNK-injected rat). Arrows indicate surrounding mononuclear cells expressing pY397-FAK. Original magnification: $\times 100$. *g*, Immunoblotting analysis demonstrated the expression of FRNK protein in the joint on day 7 after adv-FRNK injection. *h*, On days 7, 14, 21, and 28, hind paws were immersed into the chamber up to the anatomic hair line, and edema measurements were made with a volumetric apparatus. Data are shown as the mean \pm SD (*, $p < 0.05$). *i*, On day 28, the number of TRAP-positive cells was calculated in three sections from three different specimens in each group. Five visual fields were randomly selected in the each section, and the number of TRAP-positive cells were counted under a microscope. Data are shown as the mean \pm SD (*, $p < 0.01$). *j*, For radiological examination, both hind paws of each rat were dissected on day 28 and examined by soft x-ray. The evaluations were performed blindly by the same observer. A 0–3 subjected grading scale (0 = normal, 1 = mild, 2 = moderate, 3 = severe) was used to evaluate four different parameters including joint space narrowing, subchondral bone erosion, osteoporosis, and periosteal new bone formation. The radiological score refers to the sum of the subjective scores for each of these four parameters (maximum 12). Data are shown as the mean \pm SD (*, $p < 0.01$).

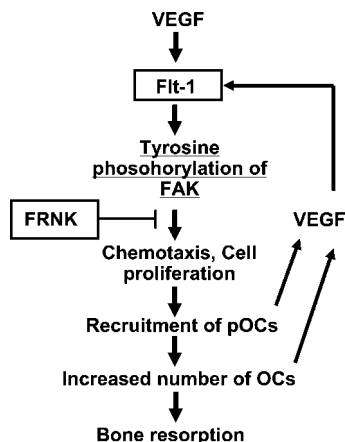


FIGURE 9. Involvement of the VEGF-Flt-1-FAK pathway in pOCs in arthritic joints.

monocyte/pOCs in the joint (42). Therefore, adv-FRNK may exert its effect by inhibiting the extracellular matrix-integrin-FAK signaling in pOCs, and further investigation is needed to show the direct link between VEGF and FAK in the arthritic joints.

In conclusion, we indicate a linear signal transduction pathway of VEGF in pOCs in arthritic joints; VEGF ligates to its receptor Flt-1, resulting in the tyrosine phosphorylation of FAK, subsequently inducing chemotaxis and cell proliferation as summarized in Fig. 9.

Acknowledgments

We thank Dr. A. M. Samarel for supplying the adenoviral vector expressing Adv-FRNK. We also thank Drs. H. Shimokawa, H. Sakai, A. Matsuo, and M. Tamura for their help with these experiments.

References

- Koch, A. E., L. A. Harlow, G. K. Haines, E. P. Amento, E. N. Unemori, W. L. Wong, R. M. Pope, and N. Ferrara. 1994. Vascular endothelial growth

- factor: a cytokine modulating endothelial function in rheumatoid arthritis. *J. Immunol.* 152:4149.
2. Lu, J., T. Kasama, K. Kobayashi, Y. Yoda, F. Shiozawa, M. Hanyuda, M. Negishi, H. Ide, and M. Adachi. 2000. Vascular endothelial growth factor expression and regulation of murine collagen-induced arthritis. *J. Immunol.* 164:5922.
 3. Sone, H., Y. Kawakami, M. Sakauchi, Y. Nakamura, A. Takahashi, H. Shimano, Y. Okuda, T. Segawa, H. Suzuki, and N. Yamada. 2001. Neutralization of vascular endothelial growth factor prevents collagen-induced arthritis and ameliorates established disease in mice. *Biochem. Biophys. Res. Commun.* 281:562.
 4. Engsig, M. T., Q. J. Chen, T. H. Vu, A. C. Pedersen, B. Therkidsen, L. R. Lund, K. Henriksen, T. Lenhard, N. T. Foged, Z. Werb, and J. M. Delaisse. 2000. Matrix metalloproteinase 9 and vascular endothelial growth factor are essential for osteoclast recruitment into developing long bones. *J. Cell Biol.* 151:879.
 5. Millauer, B., S. Witzmann-Voos, H. Schnurch, R. Martinez, N. P. Moller, W. Risau, and A. Ullrich. 1993. High affinity VEGF binding and developmental expression suggest Flk-1 as a major regulator of vasculogenesis and angiogenesis. *Cell* 72:835.
 6. Ferrara, N. 1999. Role of vascular endothelial growth factor in the regulation of angiogenesis. *Kidney Int.* 56:794.
 7. Clauss, M., H. Weich, G. Breier, U. Knies, W. Rockl, J. Waltenberger, and W. Risau. 1996. The vascular endothelial growth factor receptor Flt-1 mediates biological activities: implications for a functional role of placenta growth factor in monocyte activation and chemotaxis. *J. Biol. Chem.* 271:17629.
 8. Barleon, B., S. Sozzani, D. Zhou, H. A. Weich, A. Mantovani, and D. Marme. 1996. Migration of human monocytes in response to vascular endothelial growth factor (VEGF) is mediated via the VEGF receptor flt-1. *Blood* 87:3336.
 9. Hiratsuka, S., O. Minowa, J. Kuno, T. Noda, and M. Shibuya. 1998. Flt-1 lacking the tyrosine kinase domain is sufficient for normal development and angiogenesis in mice. *Proc. Natl. Acad. Sci. USA* 95:9349.
 10. Hanks, S. K., M. B. Calalb, M. C. Harper, and S. K. Patel. 1992. Focal adhesion protein-tyrosine kinase phosphorylated in response to cell attachment to fibronectin. *Proc. Natl. Acad. Sci. USA* 89:8487.
 11. Matsumoto, Y., K. Tanaka, K. Harimaya, F. Nakatani, S. Matsuda, and Y. Iwamoto. 2001. Small GTP-binding protein, Rho, both increased and decreased cellular motility, activation of matrix metalloproteinase 2 and invasion of human osteosarcoma cells. *Japan J. Cancer Res.* 92:429.
 12. Sieg, D. J., C. R. Hauck, D. Ilic, C. K. Klingbeil, E. Schaefer, C. H. Damsky, and D. D. Schlaepfer. 2000. FAK integrates growth-factor and integrin signals to promote cell migration. *Nat. Cell Biol.* 2:249.
 13. Maru, Y., S. K. Hanks, and M. Shibuya. 2001. The tubulogenic activity with an activated form of Flt-1 kinase is dependent on focal adhesion kinase. *Biochim. Biophys. Acta* 1540:147.
 14. Linton, S. M., A. S. Williams, I. Dodd, R. Smith, B. D. Williams, and B. P. Morgan. 2000. Therapeutic efficacy of a novel membrane-targeted complement regulator in antigen-induced arthritis in the rat. *Arthritis Rheum.* 43:2590.
 15. Horner, A., S. Bord, A. W. Kelsall, N. Coleman, and J. E. Compston. 2001. Tie2 ligands angiopoietin-1 and angiopoietin-2 are coexpressed with vascular endothelial cell growth factor in growing human bone. *Bone* 28:65.
 16. Graf, J., Y. Iwamoto, M. Sasaki, G. R. Martin, H. K. Kleinman, F. A. Robey, and Y. Yamada. 1987. Identification of an amino acid sequence in laminin mediating cell attachment, chemotaxis, and receptor binding. *Cell* 48:989.
 17. Harimaya, K., K. Tanaka, Y. Matsumoto, H. Sato, S. Matsuda, and Y. Iwamoto. 2000. Antioxidants inhibit TNF α -induced motility and invasion of human osteosarcoma cells: possible involvement of NF κ B activation. *Clin. Exp. Metastasis* 18:121.
 18. Postlethwaite, A. E., R. Snyderman, and A. H. Kang. 1976. The chemotactic attraction of human fibroblasts to a lymphocyte-derived factor. *J. Exp. Med.* 144:1188.
 19. Govindarajan, G., D. M. Eble, P. A. Lucchesi, and A. M. Samarel. 2000. Focal adhesion kinase is involved in angiotensin II-mediated protein synthesis in cultured vascular smooth muscle cells. *Circulation Res.* 87:710.
 20. Eble, D. M., J. B. Strait, G. Govindarajan, J. Lou, K. L. Byron, and A. M. Samarel. 2000. Endothelin-induced cardiac myocyte hypertrophy: role for focal adhesion kinase. *Am. J. Physiol.* 278:H1695.
 21. Takayanagi, H., T. Juji, T. Miyazaki, H. Iizuka, T. Takahashi, M. Isshiki, M. Okada, Y. Tanaka, Y. Koshihara, H. Oda, et al. 1999. Suppression of arthritic bone destruction by adenovirus-mediated *csk* gene transfer to synoviocytes and osteoclasts. *J. Clin. Invest.* 104:137.
 22. Nakagawa, N., M. Kinosaki, K. Yamaguchi, N. Shima, H. Yasuda, K. Yano, T. Morinaga, and K. Higashio. 1998. RANK is the essential signaling receptor for osteoclast differentiation factor in osteoclastogenesis. *Biochem. Biophys. Res. Commun.* 253:395.
 23. Hsu, H., D. L. Lacey, C. R. Dunstan, I. Solovyyev, A. Colombero, E. Timms, H. L. Tan, G. Elliott, M. J. Kelley, I. Sarosi, et al. 1999. Tumor necrosis factor receptor family member RANK mediates osteoclast differentiation and activation induced by osteoprotegerin ligand. *Proc. Natl. Acad. Sci. USA* 96:3540.
 24. Steven, S. W., T. Michael, W. H. Wang, and F. P. Ross. 2001. Receptor activator of nuclear factor- κ B in osteoclast precursors. *Endocrinology* 142:1290.
 25. Paavola, C. D., S. Hemmerich, D. Grunberger, I. Polsky, A. Bloom, R. Freedman, M. Mulkins, S. Bhakta, D. McCarley, L. Wiesent, et al. 1998. Monomeric monocyte chemoattractant protein-1 (MCP-1) binds and activates the MCP-1 receptor CCR2B. *J. Biol. Chem.* 273:33157.
 26. Duong, L. T., P. T. Lakkakorpi, I. Nakamura, M. Machwate, R. M. Nagy, and G. A. Rodan. 1998. PYK2 in osteoclasts is an adhesion kinase, localized in the sealing zone, activated by ligation of $\alpha_v\beta_3$ integrin, and phosphorylated by *src* kinase. *J. Clin. Invest.* 102:881.
 27. Li, X., D. Hunter, J. Morris, J. S. Haskill, and H. S. Earp. 1998. A calcium-dependent tyrosine kinase splice variant in human monocytes: activation by a two-stage process involving adherence and a subsequent intracellular signal. *J. Biol. Chem.* 273:9361.
 28. Calalb, M. B., T. R. Polte, and S. K. Hanks. 1995. Tyrosine phosphorylation of focal adhesion kinase at sites in the catalytic domain regulates kinase activity: a role for *src* family kinases. *Mol. Cell. Biol.* 15:954.
 29. Owen, J. D., P. J. Ruest, D. W. Fry, and S. K. Hanks. 1999. Induced focal adhesion kinase (FAK) expression in FAK-null cells enhances cell spreading and migration requiring both auto and activation loop phosphorylation sites and inhibits adhesion-dependent tyrosine phosphorylation of Pyk2. *Mol. Cell. Biol.* 19:4806.
 30. Chantry, D., A. Vojtek, A. Kashishian, D. A. Holtzman, C. Wood, P. W. Gray, J. A. Cooper, and M. F. Hoekstra. 1997. p110 δ , a novel phosphatidylinositol 3-kinase catalytic subunit that associates with p85 and is expressed predominantly in leukocytes. *J. Biol. Chem.* 272:19236.
 31. Schlaepfer, D. D., S. K. Hanks, T. Hunter, and P. van der Geer. 1994. Integrin-mediated signal transduction linked to Ras pathway by GRB2 binding to focal adhesion kinase. *Nature* 372:786.
 32. Schlaepfer, D. D., K. C. Jones, and T. Hunter. 1998. Multiple Grb2-mediated integrin-stimulated signaling pathways to ERK2/mitogen-activated protein kinase: summation of both c-Src- and focal adhesion kinase-initiated tyrosine phosphorylation events. *Mol. Cell. Biol.* 18:2571.
 33. Hentunen, T. A., S. H. Jackson, H. Chung, S. V. Reddy, J. Lorenzo, S. J. Choi, and G. D. Roodman. 1999. Characterization of immortalized osteoclast precursors developed from mice transgenic for both Bcl-x $_L$ and simian virus 40 large T antigen. *Endocrinology* 140:2954.
 34. Ben-Av, P., L. J. Crofford, R. L. Wilder, and T. Hla. 1995. Induction of vascular endothelial growth factor expression in synovial fibroblasts by prostaglandin E and interleukin-1: a potential mechanism for inflammatory angiogenesis. *FEBS Lett.* 372:83.
 35. Kobayashi, K., N. Takahashi, E. Jimi, N. Udagawa, M. Takami, S. Kotake, N. Nakagawa, M. Kinosaki, K. Yamaguchi, N. Shima, et al. 2000. Tumor necrosis factor α stimulates osteoclast differentiation by a mechanism independent of the ODF/RANKL-RANK interaction. *J. Exp. Med.* 191:275.
 36. Koide, M., Y. Murase, K. Yamato, T. Noguchi, N. Okahashi, and T. Nishihara. 1999. Bone morphogenetic protein-2 enhances osteoclast formation mediated by interleukin-1 α through upregulation of osteoclast differentiation factor and cyclooxygenase-2. *Biochem. Biophys. Res. Commun.* 259:97.
 37. Fuller, K., J. M. Owens, C. J. Jagger, A. Wilson, R. Moss, and T. J. Chambers. 1993. Macrophage colony-stimulating factor stimulates survival and chemotactic behavior in isolated osteoclasts. *J. Exp. Med.* 178:1733.
 38. Ogawa, S., A. Oku, A. Sawano, S. Yamaguchi, Y. Yazaki, and M. Shibuya. 1998. A novel type of vascular endothelial growth factor, VEGF-E (NZ-7 VEGF), preferentially utilizes KDR/Flk-1 receptor and carries a potent mitotic activity without heparin-binding domain. *J. Biol. Chem.* 273:31273.
 39. Robin, A. G., K. Jahangir, J. Haiyan, and Z. Ian. 2001. Src mediates stimulation by endothelial growth factor of the phosphorylation of focal adhesion kinase at tyrosine 861, and migration and anti-apoptosis in endothelial cells. *Biochem. J.* 360:255.
 40. Tanaka, S., T. Takahashi, H. Takayanagi, T. Miyazaki, H. Oda, K. Nakamura, H. Hirai, and T. Kurokawa. 1998. Modulation of osteoclast function by adenovirus vector-induced epidermal growth factor receptor. *J. Bone Mineral Res.* 13:1714.
 41. Lin, T. H., C. Rosales, K. Mondal, J. B. Bolen, S. Haskill, and R. L. Juliano. 1995. Integrin-mediated tyrosine phosphorylation and cytokine message induction in monocytic cells: a possible signaling role for the Syk tyrosine kinase. *J. Biol. Chem.* 270:16189.
 42. Sarkissian, M., and R. Lafyatis. 1999. Integrin engagement regulates proliferation and collagenase expression of rheumatoid synovial fibroblasts. *J. Immunol.* 162:1772.